J. Physiol. (1981), **312**, *pp.* 17–27
With 4 text-figures
Printed in Great Britain

IMPEDANCE OF THE AMPHIBIAN LENS

BY G. DUNCAN, L. PATMORE* AND P. B. PYNSENT
From the School of Biological Sciences, University of East Anglia, Norwich NR4 7TJ

(*Received 21 May 1980*)

SUMMARY

1. The electrical resistance of the perfused frog lens was measured using separate internal current passing and voltage measuring electrodes.

2. The resistance values obtained using voltage clamp and direct and alternating current techniques were in good agreement.

3. The voltage transients induced in response to current steps were multi-exponential in form. Increasing the external K concentration reduced both the amplitude of the voltage response and the rise time.

4. The impedance characteristics were investigated in more detail using alternating current analysis techniques.

5. In an equivalent-circuit modelling study it was assumed that there were two major pathways for current flow in the lens. The first through the surface membranes and the second through the inner fibre membranes via the narrow extracellular spaces.

6. The experimental impedance loci could not be adequately fitted by a simple two time constant model and a third time constant was introduced which may represent diffusion polarization effects in the extracellular spaces.

7. The three time constant model gave good and consistent fits to impedance data from a number of preparations.

8. The form of the impedance loci was also dependent on the external K concentration, but the only fitted parameter which changed consistently with external K was the surface membrane resistance (R_s).

INTRODUCTION

The lens is a transparent, multicellular structure comprising tightly packed fibre cells bounded at the anterior surface by a simple cuboid epithelium. Cohen (1965) pointed out that the membranes of adjacent fibres were connected by junctional complexes and more recent studies have characterized these as gap junctions (Caspar, Goodenough, Makowski & Phillips,1977). Both electrophysiological (Duncan, 1969, 1974) and dye-injection (Rae, 1974) investigations have shown that the fibre cells are functionally coupled.

Eisenberg & Rae (1976) were the first to model lens impedance using an analysis of the voltage transients in response to direct current pulses (current-clamp). In a

* Present address: Syntex Research Centre, Heriot-Watt University, Riccarton, Edinburgh EH14 4AS.

0022-3751/81/4160-0990 $07.50

later study (Mathias, Rae & Eisenberg, 1979) they applied Fourier analysis methods to the responses from white-noise injected currents. They developed a model with several elements (Fig. 1*a*) consisting of a bulk resistance (R_o) and two RC networks representing current flow through the surface and inner fibre membranes. This latter model is taken as the starting point for the present impedance study which is based on a.c. analysis methods. Since it has recently been shown that the d.c. conductance (Patmore & Duncan, 1979, 1980) and a.c. impedance characteristics (Duncan & Patmore, 1979) of lens membranes are extremely sensitive to changes in external K, we tested the model over a wide range of K concentrations. It was found necessary to introduce a third time constant into the model in order to obtain a good fit to impedance data at any K concentration.

As many methods have been used to obtain estimates of lens resistance, with sometimes quite different conclusions drawn from the data obtained (Duncan, 1969; Rae & Blankenship, 1973; Mathias *et al.* 1979), we first verified that the lens resistances obtained from three standard procedures, namely current clamp, voltage clamp and a.c. analysis, gave consistent results.

METHODS

Preparation

The lens of the Northern Leopard frog *Rana pipiens* was used in these experiments. Healthy specimens 13–20 cm in length were pithed and the whole eye removed from the head. The lens was dissected by a posterior approach. The globe was bisected revealing the posterior surface of the lens. The suspensory ligaments were cut and the lens lifted free with a glass loop. Adhering suspensory ligaments were trimmed away as much as possible but complete removal was avoided. A lens which appeared cloudy or damaged in any way through dissection was discarded. The lens was transferred to a 1 cm^3 chamber and perfused with Ringer solution at a flow rate of 2 cm^3 min^{-1} at 18 °C. The composition of the perfusate was as follows: NaCl, 105 mM; KCl, 2·5 mM; $CaCl_2$, 2 mM; $MgSO_4$, 1·2 mM; $NaHCO_3$, 6·5 mM; HEPES, 5 mM; D-glucose, 5 mM adjusted to pH 7·4 with NaOH or HCl. The K concentration of the Ringer was increased at the expense of sodium thus keeping the sodium/potassium sum constant.

Fig. 1. *A*, two time constant equivalent circuit model representing two possible current paths through the lens.

R_o, lumped series resistance of the saline and the bulk of the tissue.

R_s, surface membrane resistance.

R_i, inner membrane resistance.

R_e, extracellular space resistance.

C_s, surface membrane capacitance.

C_i, inner membrane capacitance.

The current flows from the micro-electrode inside a fibre cell to the bathing medium via one of two pathways: (1) from fibre to fibre cell via the communicating gap junctions (Duncan, 1974) and then through the surface membranes of the outer fibre cells, or (2) across the inner membranes and through the tortuous extracellular space (see also Fig. 1*C*). *B*, three time constant equivalent circuit model. A further element has been incorporated (C_d and R_d) which describes the resistance and capacitance of unstirred layers in the extracellular space. This is in series with the inner membrane element. *C*, diagrammatic representation of possible pathways for current flow between the lens cytoplasm and bath. Current flowing through the narrow extracellular spaces (pathway 2) would be expected to encounter the unstirred layer elements C_d and R_d (see also Fig. 1*B*).

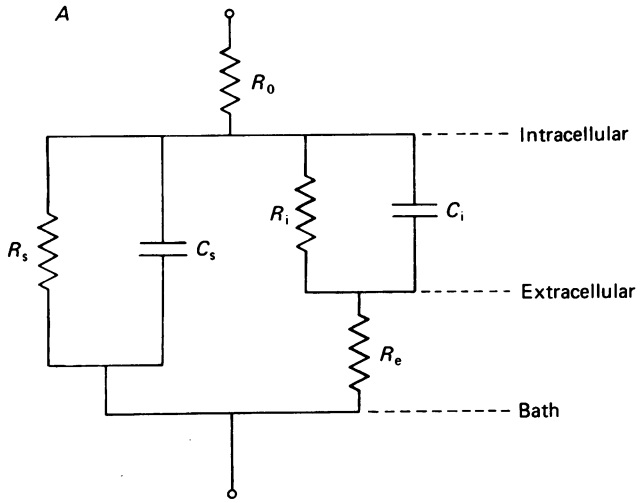
A
R_0
Intracellular
R_i
C_i
R_s
C_s
Extracellular
R_e
Bath

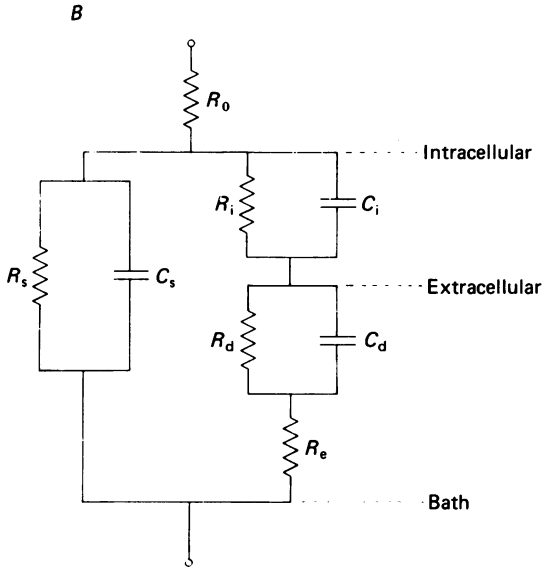
B
R_0
Intracellular
R_i
C_i
R_s
C_s
Extracellular
R_d
C_d
R_e
Bath

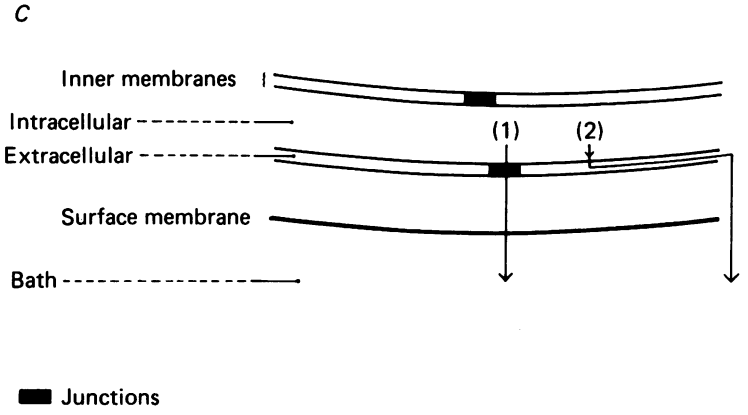
C
Inner membranes
Intracellular
Extracellular
(1)
(2)
Surface membrane
Bath
Junctions

Electrical recording

A two internal micro-electrode technique was used to measure lens impedance similar to that described by Duncan (1969) and Delamare & Duncan (1977). Micro-electrodes were pulled from thin walled filament glass tubing (Clarke Electromedical, Pangbourne, U.K) and filled with 3M-KCl. The tip resistances were between 1–5 MΩ. These low resistance electrodes were essential in the impedance analysis (see below) as they gave a negligible contribution to the resistance and reactance measurements at the frequencies used (Falk & Fatt, 1964).

The lens potential was measured between an internal micro-electrode and a Ringer-agar reference electrode on which the lens was seated. These were connecred to a high impedance differential amplifier (Model 750, WPI Inc.) and the output displayed on a dual beam storage oscilloscope (Tekronix, Model 5013). The oscilloscope was connected to an FM tape recorder (Tandberg Instrumentation, model 100) and a chart recorder (Bryans Southern, 1800). Lens impedance was measured by passing current from a second internal microelectrode to a virtual earth electrode in the chamber and monitoring the response of the previous electrode pair. The virtual earth electrode consisted of a silver/silver chloride wire connected to earth via a current-to-voltage transducer. The output from this device, connected to the second oscilloscope channel, gave an accurate measure of the current passed through the lens.

Step pulses or sine waves (0·01–100 Hz) of current were delivered from a current injection amplifier (model 701, WPI Inc.) and their magnitude and duration were controlled by a square-wave (Tekronix, 2601) or sine-wave generator (Wavetek, 180) respectively.

Signal processing of sinusoidal currents

Lissajou figures were reconstructed on the storage screen of the oscilloscope operating in the $X-Y$ mode and resistive (R) and reactive (X) components of the impedance were calculated as described by Smith (1971). Impedance loci (Cole, 1968) were generated from the data obtained in a range of external K concentations.

Equivalent circuit models

The theoretical impedance of an equivalent circuit can be computed by assessing the impedance (Z) of each component.

For the two time constant model shown in Fig. 1*A*, the admittance ($1/Z$) is given by

$$Y = \frac{1}{R_s} + j\omega C_s + \left[R_e + \left(\frac{1}{R_i} + j\omega C_i \right)^{-1} \right]^{-1}, \tag{1}$$

where j is the imaginary operator and ω the angular frequency ($\omega = 2\pi f$). This expression has real and imaginary parts which when grouped together can be arranged in the form

$$Y = B + jD \tag{2}$$

therefore

$$Z = \frac{1}{B+jD} = \frac{B-jD}{B^2+D^2}. \tag{3}$$

Thus the real component of the impedance is given by

$$R = \frac{B}{B^2+D^2}, \tag{4}$$

and the imaginary component by

$$X = \frac{-D}{B^2+D^2}. \tag{5}$$

The same treatment was applied to calculate the theoretical impedance of the three time constant model (Fig. 1*B*). This takes into account the impedance of the unstirred layer in the extracellular space. In this case

$$Y = \frac{1}{R_s} + j\omega C_s + \left[\left(\frac{1}{R_d} + j\omega C_d \right)^{-1} + \left(\frac{1}{R_i} + j\omega C_i \right)^{-1} + R_e \right]^{-1}, \tag{6}$$

with R and X calculated as before.

The impedance loci predicted by these two models were fitted to the experimental data using an iterative technique (NAG, 1977) based on Powell's method (1968). The routine optimised the parameters of the model to data presented as a set of resistance and reactance values over the experimental range of frequencies.

RESULTS

The three different methods used to obtain estimates of the over-all resistance of the lens gave very similar results in the four preparations studies (Table 1). The values, which ranged from 8·2 to 13·2 kΩ, were similar to those reported previously for frog obtained by current clamp (Duncan, 1969; Eisenberg & Rae, 1976) and noise analysis methods (Mathias *et al.* 1979).

TABLE 1. Comparison of lens resistance measurements

Experiment no.	Measured resistance (kΩ)		
	$R_{d.c.}$	$R_{a.c.}$	$R_{v.c.}$
781012	11·3	11·1	10·8
781103	8·3	8·2	8·6
781130	9·7	9·6	10·0
781208	13·2	12·8	13·1

The resistance values in the current-clamp ($R_{d.c.}$) and voltage-clamp ($R_{v.c.}$) experiments were obtained from the steady-state voltage or current transient respectively. The a.c. resistance values ($R_{a.c.}$) were obtained by extrapolating the impedance data points to their intercept with the resistance axis in the impedance loci.

A typical voltage response to a step of curent is shown in Fig. 2*A*, and the relatively long time constant of the response has previously been remarked upon by Eisenberg & Rae (1976). Plotting the relaxation of the voltage against time (semilog plot) shows that the response is multi-exponential in nature (Fig. 2*B*). Increasing the external K concentration not only decreases the magnitude of the response (Patmore & Duncan, 1979 and Fig. 2*A*) but also changes the relaxation rate.

It is obviously of interest to know whether all the amplitude and rate proceses are affected equally on increasing external potassium and if they are not, which of the impedance elements are affected most. In order to investigate this in greater detail the a.c. method was used (see also Clausen, Lewis & Diamond, 1979). A typical impedance locus mapped out with the lens perfused with 2·5 mM-K Ringer is shown in Fig. 3*A* and the continuous line gives the best fit generated by the two time-constant model (Fig. 1*A*). The fit can be considerably improved if a third time constant is added to the model (Fig. 3*B*). The fitting technique was applied to the impedance loci derived from a number of lenses and the fitted parameters are given in Table 2*A*. It should be noted that because two of the RC elements are in series, the fitting routine cannot distinguish between the elements $R_i C_i$ and $R_d C_d$. This is obvious from eqn. (6). We have therefore followed the convention of attributing the higher resistance value to R_i. The resistances associated with each of the putative membrane elements are in the order $R_s > R_i > R_d$, while the capacitances C_i and C_d are approximately 10 times greater than the capacitance associated with the surface membranes. The predicted over-all resistance $R_{a.c.}$ of each of the preparations was in agreement with the total

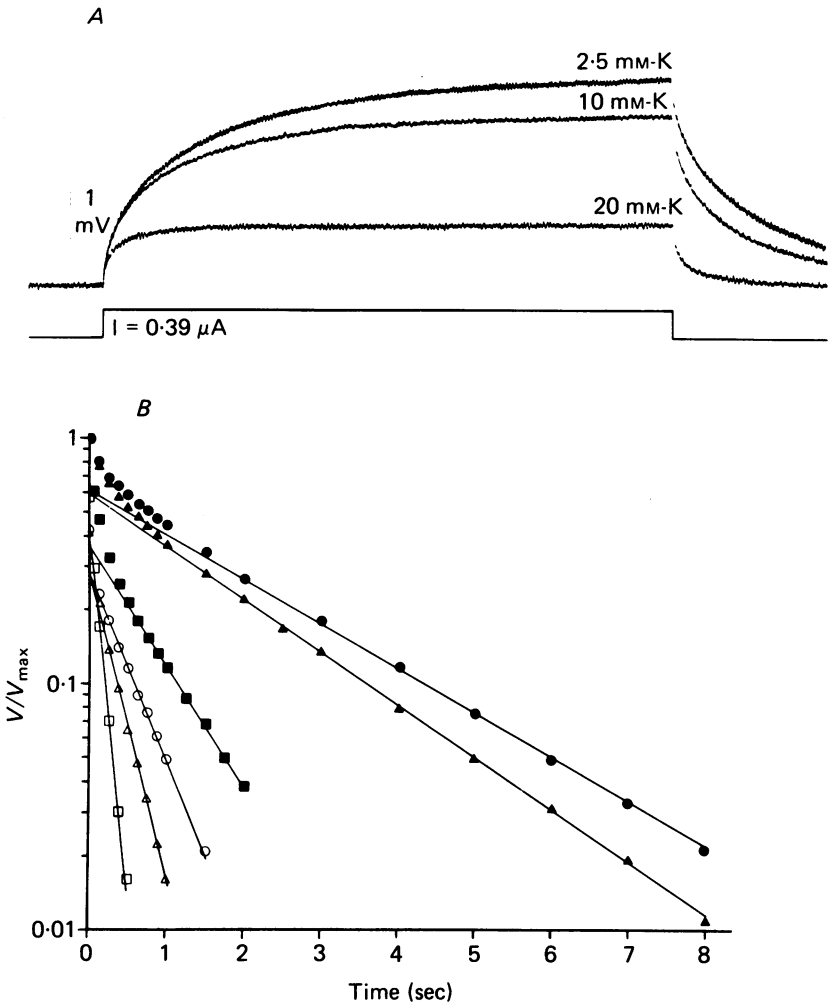

Fig. 2*A*, voltage response of the frog lens potential to a step pulse of current at three levels of external potassium. The current pulse is 10 sec in duration. *B*, voltage relaxations from Fig. 2*A* replotted on a logarithmic scale. ● 2·5 mM-K^+; ▲ 10 mM-K^+; ■ 20 mM-K^+; V_{max} is the 'steady state' voltage and V the voltage at some time after the current is removed. The lines through the filled symbols give an estimate of the slow component of each response. The fast component (open symbols) was generated by subtracting the slow component from the original response.

resistance $R_{d.c.}$ estimated by applying current steps to the same preparations. These lenses were also perfused with Ringer solutions in which the potassium concentration was increased from 2·5 to 25 mM. The corresponding impedance loci were generated and the three time constant model was fitted to these data. The resulting computed parameters are shown in Table 2*B*. The only parameter which changes consistently for each lens on increasing the external K is R_s (compare Table 2, parts *A* and *B*).

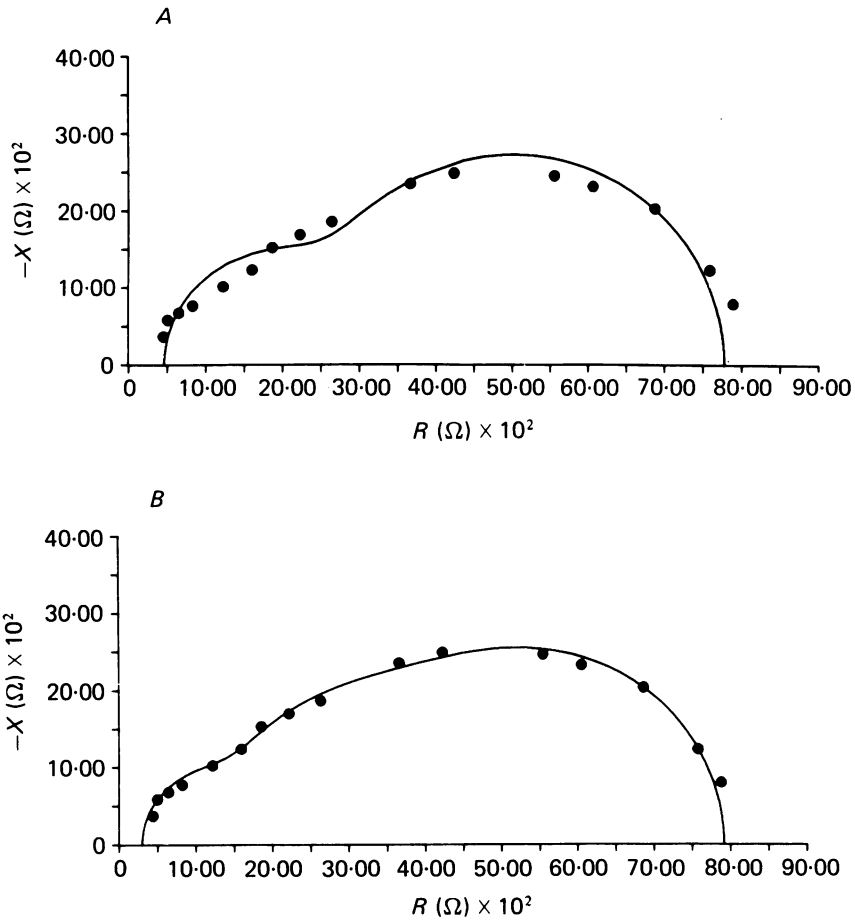

Fig. 3*A*, impedance locus mapped out in normal (2·5 mM-K) Ringer solution. The continuous line is the best fit of the two time constant model (see Fig. 1*A*) to the data points. The parameter values obtained were as follows:

$$R_o = 3{\cdot}00 \times 10^2\,\Omega;\quad R_e = 4{\cdot}78 \times 10^3\,\Omega;\quad R_s = 7{\cdot}37 \times 10^3\,\Omega$$
$$R_i = 1{\cdot}00 \times 10^7\,\Omega;\ C_s = 3{\cdot}86 \times 10^{-5}\,\text{F and } C_i = 9{\cdot}97 \times 10^{-5}\,\text{F}.$$

In this experiment the frequencies ranged from 0·01 to 40 Hz (see also Fig. 4). *B*, best fit of the three time constant model (see Fig. 1*B*) to the same impedance data. The parameters values obtained were as follows:

$$R_o = 3{\cdot}00 \times 10^2\,\Omega;\ R_e = 1{\cdot}84 \times 10^3\,\Omega;\ R_s = 18{\cdot}10 \times 10^3\,\Omega;$$
$$R_i = 8{\cdot}46 \times 10^3\,\Omega;\ R_d = 1{\cdot}91 \times 10^3\,\Omega;\ C_s = 0{\cdot}021\,\text{mF}$$
$$C_i = 0{\cdot}218\,\text{mF and } C_d = 0{\cdot}108\,\text{mF}.$$

Impedance loci were also mapped out over a range of external K concentrations from 2·5 to 40 mM-K and good fits were obtained in all cases using the three time constant model (Fig. 4). Again R_s was the only parameter which changed consistently with increasing external potassium. A decrease in R_s was always obtained.

TABLE 2*A*, fitted parameter values obtained in normal (2·5 mM) K solution

Lens	R_o	R_e	R_s	R_i	R_d	C_s	C_i	C_d	$R_{a.c.}$	$R_{d.c.}$
1	0·14	2·74	29·5	9·74	3·03	0·036	0·303	0·120	10·30	12·73
2	0·88	2·13	12·9	11·26	2·80	0·017	0·215	0·079	8·06	9·45
3	0·90	2·14	14·6	6·29	1·75	0·031	0·360	0·173	6·90	7·95
4	0·87	2·22	15·2	5·50	2·81	0·020	0·318	0·089	7·09	8·29
5	0·63	2·33	61·3	5·92	2·32	0·023	0·307	0·087	9·65	10·72
6	0·34	1·60	11·1	7·33	2·01	0·040	0·271	0·187	5·85	—
Mean	0·63	2·18	24·1	7·67	2·45	0·028	0·296	0·123	7·98	9·83
±S.E. of mean	0·13	0·15	7·9	1·15	0·21	0·004	0·020	0·019	0·70	0·87

The units of resistance and capacitance are kΩ and mF respectively.

B, fitted parameter values obtained in high (25 mM) K solution.

Lens	R_o	R_e	R_s	R_i	R_d	C_s	C_i	C_d	$R_{a.c.}$	$R_{d.c.}$
1	0·37	2·24	2·21	8·27	1·91	0·066	0·395	0·137	2·25	3·21
2	0·79	1·87	4·37	17·7	3·41	0·015	0·155	0·063	4·46	5·10
3	0·59	1·32	3·11	3·08	1·56	0·014	0·385	0·068	2·63	3·15
4	0·82	2·26	3·90	8·51	3·68	0·021	0·853	0·097	3·89	4·09
5	0·33	0·74	8·86	0·86	0·48	0·013	0·219	0·048	2·01	2·38
6	0·19	1·16	2·02	28·5	6·22	0·043	0·472	0·130	2·10	—
Mean	0·52	1·60	4·08	11·15	2·88	0·029	0·414	0·091	2·89	3·59
±S.E. of mean	0·11	0·25	1·03	3·88	0·83	0·009	0·10	0·02	0·42	0·46

The parameters are defined in Fig. 1*B*. $R_{a.c.}$ is the predicted resistance between the lens interior and bathing solution given by eqn. (4) when ω equals zero. $R_{d.c.}$ is the resistance measured using the current-clamp method.

DISCUSSION

From the current clamp data presented in Fig. 2 and the a.c. results shown in Figs. 3 and 4 it is clear that the over-all impedance of the frog lens comprises a number of elements. Duncan & Delamare (1978) and Mathias *et al.* (1979) have suggested that two current paths should be considered in an analysis of lens impedance, namely that through the inner membranes and extracellular space in the bulk of the lens as well as the more obvious intracellular route through gap junctions and across the surface fibre membranes (Fig. 1*C*).

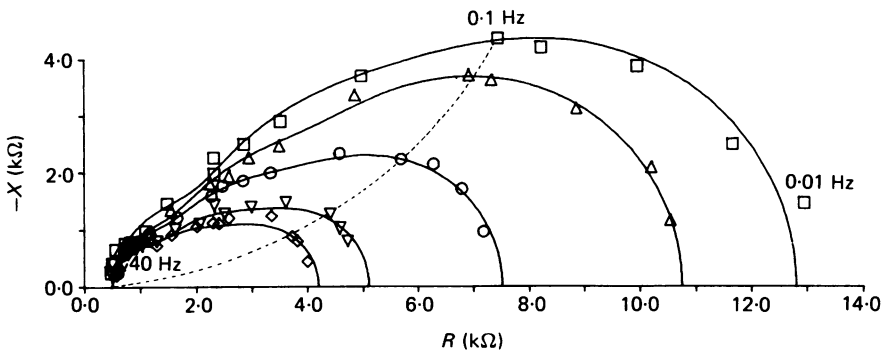

Fig. 4. The effect of external potassium concentrations on lens impedance. □ 2·5 mM-K; △ 5 mM-K; ○ 10 mM-K; ▽ 20 mM-K; ◇ 40 mM-K. The continuous lines are the 'best fits' to the data points generated from the three time constant model. The fitted values for R_s were 98·6, 96·7, 24·2, 9·62 and $7{\cdot}63 \times 10^3\ \Omega$ respectively. The fitted values for the other parameters did not change significantly throughout the range. The frequencies used ranged from 0·01 to 40 Hz and the dashed curve joins the points at 0·1 Hz for the individual loci generated at the different K concentrations.

In their detailed study Mathias *et al.* (1979) found that a simple two element model (Fig. 1*A*) was not sufficient to explain all of their data. In extending their theory to a distributed equivalent circuit model, they in effect introduced a third time constant by assuming that the length constant (λ) of the lens was frequency dependent (Mathias *et al.* (1979), Table 1). They did not in fact test their assumption, which could be done by simply measuring the frequency response to their injected current noise at different electrode separations. Patmore (1979), however, has tested this in a series of a.c. experiments. He found that any differences in a.c. – generated impedance loci obtained at different electrode separations could be explained entirely by a change in R_o alone (Fig. 1*A*).

We have therefore assumed that there is a second time-constant associated with the inner fibre membranes (R_d and C_d of Fig. 1*B*) which could, for example, represent diffusion polarization effects in the unstirred layers of the narrow extracellular spaces of the lens (Fig. 1*C*). Such an element has previously been invoked by Rehm and co-workers to explain long time constant voltage transients in frog cornea and gastric mucosa (Kidder & Rehm, 1970; Rehm, Shoemaker, Sanders, Tarvin, Write & Friday, 1973).

The response time of the frog lens membrane potential following a current step (Fig. 2*A*) is relatively long and hence it is not surprising that the time constants of the individual elements defined in Fig. 1*B* are also long. The RC products for the surface membranes, inner membranes and diffusion polarization effects are 0·67, 2·3 and 0·3 sec respectively (computed from the parameters given in Table 2*A*). If we assume that the capacitance associated with the surface and inner membrane systems is of the order of 1 μF cm^{-2} then the associated resistances are 0·67 and 2·3 MΩ cm^2 respectively. These resistance values are quite different from those derived by Mathias *et al.* (1979). They applied similar arguments to their modelling data and concluded that the resistance of the surface membranes was 5 kΩ Cm^2 while the resistance of the inner membranes was 2 MΩ cm^2. The difference between the two approaches probably depends on whether basically a two or three element model is chosen for data fitting. The best fits to the two time constant model (fig. 3*A*) obtained with the present data in fact yield parameter estimates that are quite close to those obtained by Mathias *et al.* (1979). The fitted parameters of the two time constant model require the resistance contribution from the inner membranes to be approximately one thousand times greater than the surface membrane contribution. The parameters deduced from the three time constant model however (Fig. 3*B* and Table 2*A*) indicate that the surface membranes actually contribute more to the overall measured resistance than the inner membranes.

Characteristic time constants of other tisues range from 0·03 msec for the active membrane in squid nerve (Cole & Curtis, 1939) to 20 sec in frog gastric mucosa (Noyes & Rehm, 1971). Epithelial tissues tend to have longer time constants associated with their impedance. The characteristic time constant of frog skin, for example is 0·05 sec. Smith (1971) has also shown that the characteristic time constant of frog skin is dependent on the composition of the bathing solutions. In the case of the lens, because R_s is preferentially reduced in high K, the characteristic time constant of the surface membranes changes from approximately 1 sec in 2·5 mM-K to 0·1 sec in 25 mM-K. This decrease in time constant leads to the overall sharpening of the voltage transient response observed in Fig. 2*A* and *B*. Delamare & Paterson (1978) have also observed a sharpening of the DC response in low Ca solutions where a drop in resistance is observed.

Patmore & Duncan (1979, 1980) have previously suggested that the large change in membrane conductance on increasing external potassium is in fact due to the presence of voltage-sensitive K channels in the lens membranes. The result of applying modelling and curve-fitting techniques to amphibian lens impedance data suggests that the voltage-sensitive K channel system is primarily located in the surface membranes of the lens.

This research was supported by a grant from The Nuffield Foundation. L. Patmore acknowledges the receipt of an S.R.C. studentship during the course of this work.

REFERENCES

CASPAR, D. L. D., GOODENOUGH, D. A., MAKOWSKI, L. & PHILLIPS, W. C. (1977). Gap junction structures. I. Correlated electron microscopy and X-ray diffraction. *J. cell Biol.* **74**, 605–616.

CLAUSEN, C., LEWIS, S. A. & DIAMOND, J. M. (1979). Impedance analysis of a tight epithelium using a distributed resistance model. *Biophys. J.* **26**, 291–317.

COHEN, A. I. (1965). Electron microscopy of the normal human lens. *Investive Ophth.* **4**, 433–427.

COLE, K. S. (1968). In *Membranes, Ions and Impulses*, Classical biophysics. Berkeley and Los Angeles, U.S.A.: Univ. of California Press.

COLE, K. S. & CURTIS, H. J. (1939). Electrical impedance of the squid axon during activity. *J. gen. Physiol.* **22**, 649–670.

DELAMERE, N. A. & DUNCAN, G. (1977). A comparison of ion concentrations, potentials and conductances of amphibian, bovine and cephalopod lenses. *J. Physiol.* **272**, 167–186.

DELAMERE, N. A. & PATERSON, C. A. (1978). The influence of calcium-free EGTA solution upon membrane permeability in the crystalline lens of the frog. *J. gen. Physiol.* **71**, 581–593.

DELAMERE, N. A. & PATERSON, C. A. (1979). The influence of calcium-free solutions upon permeability characteristics of the rabbit lens. *Expl Eye Res.* **28**, 45–53.

DUNCAN, G. (1969). The site of the ion restricting membranes in the toad lens. *Expl Eye Res.* **8**, 406–412.

DUNCAN, G. (1974). Comparative Physiology of the lens membranes. In *The Eye*, vol. 5, pp. 357–399, ed. DAVSON, H. and GRAHAM, L. T. London: Academic.

DUNCAN, G. & DELAMERE, N. A. (1978). Electrophysiology of the mammalian lens. *Interdiscipl. Topics Geront* **12**, 278–290.

DUNCAN, G. & PATMORE, L. (1979). The effects of tetraethylammonium on the impedance of the lens of the frog, *Rana pipiens*. *J. Physiol.* **291**, 71–72.

EISENBERG, R. S. & RAE, J. L. (1976). Current voltage relationships in the crystalline lens. *J. Physiol.* **262**, 285–299.

FALK, G. & FATT, P. (1964). Linear electrical properties of striated muscle fibres observed with intracellular microelectrodes. *Proc. R. Soc.* B **160**, 69–81.

KIDDER, G. N. & REHM, W. S. (1970). A model for the long time-constant voltage response to current in epithelial tissues. *Biophys. J.* **10**, 215–236.

MATHIAS, R. T., RAE, J. L. & EISENBERG, R. S. (1979). Electrical properties of structural components of the crystalline lens. *Biophys. J.* **25**, 181–201.

N.A.G. (1977). *Fortran Library Manual (Mark 5), Routine E04FBF*. Oxford, U.K.: NAG Library Service.

NOYES, D. H. & REHM, W. S. (1971). Unstirred layer model for the long time-constant transient voltage response to current in epithelial tissues. *J. theor. Biol.* **32**, 25–45.

PATMORE, L. (1979). Electrophysiological studies on the lens. PhD Thesis, University of East Anglia, U.K.

PATMORE, L. & DUNCAN, G. (1979). A TEA-sensitive component in the conductance of a non-excitable tissue (the amphibian lens). *Expl Eye Res.* **28**, 349–352.

PATMORE, L. & DUNCAN, G. (1980). Voltage-dependent potassium channels in amphibian lens membranes: evidence from radiotracer and electrical conductance measurements. *Expl Eye Res.* **31** (in the Press).

POWELL, M. J. D. (1968). A Fortran subroutine for solving systems of non-linear algebraic equations. *Harwell report AERE–R5947*. London: H.M. Stationary Office.

RAE, J. L. (1974). The movement of procion dye in the crystalline lens. *Investiv Ophth.* **13**, 147–153.

RAE, J. L. & BLANKENSHIP, J. E. (1973). Electrical measurements in the frog lens. *Expl Eye Res.* **15**, 209–217.

REHM, W. S., SHOEMAKER, R. L., SANDERS, S. S., TARVIN, J. T., WRITE, J. A. & FRIDAY, E. A. (1973). Conductance of epithelial tissues with particular reference to the frog's cornea and gastric mucosa. *Expl Eye Res.* **15**, 533–552.

SMITH, P. G. (1971). The low frequency electrical impedance of the isolated frog skin. *Acta physiol. scand.* **81**, 355–362.